

See discussions, stats, and author profiles for this publication at: <https://www.researchgate.net/publication/245236581>

Hydrogenation of 2Butyne1,4-diol Using Novel Bio-Palladium Catalysts

ARTICLE in INDUSTRIAL & ENGINEERING CHEMISTRY RESEARCH · FEBRUARY 2010

Impact Factor: 2.59 · DOI: 10.1021/ie900663k

CITATIONS

18

READS

47

5 AUTHORS, INCLUDING:



Lucille Bodenes

Université de Pau et des Pays de l'Adour

6 PUBLICATIONS 50 CITATIONS

SEE PROFILE



J. A. Bennett

Aston University

23 PUBLICATIONS 277 CITATIONS

SEE PROFILE



Kevin Deplanche

University of Birmingham

30 PUBLICATIONS 466 CITATIONS

SEE PROFILE



Lynne E Macaskie

University of Birmingham

174 PUBLICATIONS 4,640 CITATIONS

SEE PROFILE

Hydrogenation of 2-Butyne-1,4-diol Using Novel Bio-Palladium Catalysts

Joseph Wood,^{*,†} Lucille Bodenes,^{†,§} James Bennett,[†] Kevin Deplanche,[‡] and Lynne E. Macaskie^{*}

Department of Chemical Engineering, University of Birmingham, Edgbaston, Birmingham, B15 2TT, United Kingdom, Department of Biosciences, University of Birmingham, Edgbaston, Birmingham, B15 2TT, United Kingdom, ENSIACET, 118 Route de Narbonne, 31077 Toulouse Cedex 4, France

Palladium catalyst samples were prepared upon bacterial biomass supports (Gram-positive *A. oxidans* and Gram-negative *R. capsulatus*) and tested in the partial hydrogenation of 2-butyne-1,4-diol to 2-butene-1,4-diol. The objectives of the study were to assess the effects of operating conditions in the stirred autoclave upon the reaction conversion and selectivity and to compare the biologically supported palladium (BioPd) catalyst performance with that of a conventionally supported catalyst. Variables investigated included solvent, stirring speed, and catalyst metal loading. A maximum selectivity toward 2-butene-1,4-diol of 0.98 was observed in a solvent composed of 5% isopropyl alcohol (2-propanol) in water at a conversion of 75% 2-butyne-1,4-diol for the Pd/*A. oxidans* catalyst. The Pd/*R. capsulatus* catalyst showed a maximum selectivity of 1.0 at a conversion of 62.6%. Concentration profiles of the different hydrogenation products were fitted using a Langmuir–Hinshelwood expression, which showed a higher fitted adsorption constant of 2-butyne-1,4-diol in a 5% 2-propanol/water solvent, compared with pure 2-propanol, suggesting that adsorption is stronger in the mixed solvent. At a typical catalyst loading of 0.29 g/L (Pd/*R. capsulatus*), analysis of the mass-transfer steps in the reactor showed that ~63% of the resistance to mass transfer lies at the catalyst (liquid–solid) particle and ~37% lies at the gas bubble interface. BioPd was proven to be a highly selective catalyst for partial hydrogenation reactions and has the advantage that it can be prepared inexpensively from metal-waste-bearing solutions.

1. Introduction: Novel Bio-Palladium Catalysts for Hydrogenation Reactions

Nanoparticulate palladium has received attention from researchers,^{1,2} because of its outstanding effectiveness as a catalyst, in particular for reactions such as hydrogenation and hydrogenolysis. However, the production of nanoparticles often requires expensive equipment to promote controlled particle growth. Concurrently, palladium is a valuable metal that is becoming increasingly scarce in supply, because of the demand for its use in a range of industrial processes and electronic goods, as well as automotive catalytic converters. Traditionally, the surface area of palladium metal is maximized for catalytic applications by the use of a support such as porous carbon, silica, or alumina. We have developed a technique to utilize bacteria as a precious metal catalyst support. Nanoparticulate ferromagnetic palladium clusters are incorporated within the outer cell layers of bacterial cells. The cells typically fall within the size range of 1–5 μm . Production of the biologically supported palladium (BioPd) catalyst was pioneered by the use of sulfate-reducing bacterium *Desulfovibrio desulfuricans*,³ which reduces soluble Pd(II) to Pd(0). BioPd can be utilized directly in the above form as particles, or it can take advantage of the natural ability of bacteria to form self-adhesive biofilms on structured supports before metallization, allowing the potential use of metallized cells in flow-through reactors.⁴ This production route could be used to manufacture nanoparticulate palladium catalysts scalably from metal-containing waste solutions (for example, from electronic scrap materials⁵ or spent automotive catalysts⁶). It would therefore avoid the use of new refined palladium metal and provide a low-cost route for catalyst production. BioPd thus

represents a potentially low-cost nanoparticulate catalytic material that can be manufactured from recycled materials⁶ and could offer high activity and selectivity in a range of chemical reactions of industrial significance.

Details of the manufacturing method and properties of BioPd have already been studied and published.^{3,6–8} Mabett et al.⁶ conducted transmission electron microscopy (TEM) studies on BioPd manufactured using *D. desulfuricans* after reduction of a mixed-metal solution (Pd(II), Pt(IV), Rh(III)), which showed entire cells with precipitate on the cell surface that was not visible on the otherwise untreated biomass. The precipitate was resolvable to individual particles, which were shown by energy-dispersive X-ray microanalysis to contain palladium.⁷ The crystalline nature of the material was shown by the sharp nature of the X-ray powder pattern, which confirmed the speciation as Pd(0) with Pd/*D. desulfuricans*. The manufacture of BioPd can be facilitated by the use of different strains of bacterial cells. For Pd/*D. desulfuricans*, the nanoparticles within the periplasmic space were bounded by the Gram-negative double membrane structure erupting through this to penetrate the cell surface,⁷ whereas for *B. sphaericus*, the palladium particles were shown to be located between the peptidoglycan and the S-layer of the Gram-positive cell. In both types of cells, the palladium nanoparticles were enclosed initially within the outermost cell layers.⁸ Solid-state analysis of magnetic behavior⁷ and extended X-ray absorption fine structure (EXAFS) analysis⁸ revealed that the palladium nanoparticles have sizes in the range of 1–6 nm. Bennett et al.⁹ determined via chemisorption studies that the average palladium particle size of Pd/*D. desulfuricans* is 1.7 nm. The manufacture of BioPd using bacteria requiring to be pregrown under strictly anaerobic under anaerobic conditions, such as *D. desulfuricans*, could incur costs associated with expelling traces of oxygen from the biomass growth cultures. Furthermore, the sulfate-reducing bacteria form H_2S , which is a potent catalyst poison, as a metabolic product, requiring

* To whom correspondence should be addressed. Tel.: +44 (0) 121 414 5295. Fax: +44 (0) 121 414 5324. E-mail: j.wood@bham.ac.uk.

[†] Chemical Engineering.

[‡] Biosciences.

[§] ENSIACET.

extensive washing of the cells before exposure to Pd(II). However, alternative bacterial cells such as *Arthrobacter oxidans* (Gram-positive) and *Rhodobacter Capsulatas* (Gram-negative), which may be palladized under aerobic conditions, could offer a less-expensive manufacturing solution, because they do not require special air-free conditions. Furthermore, aerobic growth of biomass typically produces higher yields and scope for high-density cultures.

Palladized bacterial cells have been demonstrated to have a high activity in a range of catalytic test reactions, such as the production of hydrogen from hypophosphite, the reductive dechlorination of polychlorinated biphenyls,^{10,11} the dehalogenation of Lindane,¹² polybrominated diphenyl ether flame retardants,¹³ and trichloroisopropyl phosphate in groundwater¹⁴ and the reduction of Cr(VI) to Cr(III).¹⁵ BioPd was also effective for use in three-phase gas–liquid–solid catalytic reactors (for example, in the hydrogenation of itaconic acid in a stirred autoclave).⁸ Two different strains of bacterial support—*D. desulfuricans* (Gram-negative) and *B. sphaericus* (Gram-positive)—were tested in the aforementioned reaction, and their performance was compared with commercial graphite-supported catalyst. For the Pd/*B. sphaericus* materials, several metal loadings upon the bacteria were tested and it was found that 2% palladium loading gave the optimum initial reaction rate. It was determined that the highest initial rates of reaction for 5% Pd/*D. desulfuricans*, 2% Pd/*B. sphaericus*, and 5% Pd/graphite were 11.0×10^{-3} , 12.0×10^{-3} , and 13.0×10^{-3} mol g-Pd⁻¹ s⁻¹ respectively, illustrating that the biologically prepared materials displayed activity similar to that of the commercial material.

Recently, BioPd has also been shown to provide selectivity toward the desirable products in a multiproduct reaction. Bennett et al.⁹ investigated the hydrogenation and isomerization of 2-pentyne using 5% BioPd and 5% Pd/Al₂O₃ catalysts. The biomass-supported catalyst compared well to the conventional inorganic supported catalyst, leading to quantitative conversions of alkyne after 5 h with maximum product ratios of pentene/pentane in the range of 8–14 and cis/trans product ratios in the range of 6–14. However, further evidence of the ability of BioPd to selectively catalyze desirable reactions, while suppressing the production of waste products, is needed to provide the first evidence of the scope for this material to be used as an alternative catalyst for industrial reactions.

The partial hydrogenation of 2-butyne-1,4-diol to 2-butene-1,4-diol is a well-studied reaction from the point of view of understanding the effects of reaction engineering upon the reaction rate and product selectivity. 2-Butene-1,4-diol is also an industrially significant product, being used in the manufacture of vitamins and endosulfan insecticide.¹⁶ Chaudhari et al.¹⁷ studied the kinetics of butynediol hydrogenation over a Pd–Zn–CaCO₃ catalyst in a batch slurry reactor, which showed that the reaction rate is proportional to the square root of hydrogen pressure and an increase in butynediol concentration inhibited the reaction. Telkar et al.¹⁸ studied the roles of ammonia, catalyst pretreatment, and kinetics, and they determined that the role of ammonia and support type was important in achieving a high selectivity toward 2-butene-1,4-diol. The reaction has also been studied in different reactor devices designed to improve hydrogen mass transport, such as the spinning basket¹⁹ and monolith bubble column.²⁰ The types of reactor and hydrodynamic conditions have been found to strongly influence the product selectivity in the reaction. Structured catalysts such as monolith and capillary reactors can lead to improved selectivity toward 2-butene-1,4-diol, because

Table 1. Experimental Parameters for the Reference Reaction

parameter	conditions used
catalyst (bacterial strain)	BioPd (<i>A. oxidans</i>)
mass of BioPd	0.100 g
mass of B3D reactant	2 g
molar ratio Pd/B3D	0.205 mol % Pd
solvent	2-propanol
temperature	40 °C
stirring speed	1000 rpm
pressure	2 bar

of the improved mass transfer of hydrogen across a film on the catalyst surface.²¹ Novel activated-carbon-fiber-supported palladium catalysts have also shown some promise for the selective hydrogenation of butynediol.^{22,23} It has been shown that the selection of solvent and composition of mixed solvents strongly influence the reaction rate.²⁴ In a mixed solvent of 2-propanol/water, the solvent composition influences the solubility of hydrogen as well as the gas bubble size. This leads to maxima in reaction rates at compositions of both 5% propanol/water and 100% propanol. Alcohol–water mixtures are known to be highly nonideal solutions, with negative excess enthalpies due to changes in the arrangement of hydrogen bonds throughout the liquid.^{25–27} Changes in hydrogen bonding may effect the interaction of substrates with each other and/or with the catalyst. This, in turn, may lead to differences in adsorption enthalpies, allow alternate reaction mechanisms to occur more favorably, and ultimately affect selectivity and the reaction rate.

The objective of this study is to report the hydrogenation of 2-butyne-1,4-diol using a BioPd catalyst, manufactured using two types of bacteria as catalyst supports. Although the selective hydrogenation of 2-butyne-1,4-diol has been previously demonstrated for a range of other supported palladium catalysts, it serves as a useful test reaction for demonstrating the activity and selectivity of the BioPd catalyst, compared to a commercial material. This work provides evidence that the BioPd catalyst is effective in catalyzing a range of multiproduct reactions, with selectivity toward the desired product.

2. Experimental Methods

Biopalladium Production. *Rhodobacter capsulatas* (ZX-5) was obtained as the waste from a biohydrogen production process and *Arthrobacter oxidans* (NCIMB 105 04) was grown from a bacterial culture. Biosupported palladium particles were prepared via the reduction of sodium tetrachloropalladate(II) on bacterial cells (*A. oxidans* NCIMB 10504 or *R. capsulatus* ZX-5) with hydrogen gas as the electron donor, using the method of Lloyd et al.³ The mass ratio of Pd(II) in solution to the dry weight of cells was adjusted depending on mass-percent loading that was required. The palladium-loaded bacterial cells were centrifuged and washed three times with distilled water and once with acetone, then dried in air, according to the methods of Creamer et al.⁸ The final material is supported on dead bacterial cells rather than live bacteria. Because palladium was not leached by washing in acetone, the bacterial cells are resistant to palladium leaching. The dried palladized biomass was determined to be ~20 times more resistant to attrition under shear than palladized fresh cells.

Hydrogenation Reactions. The reactions were conducted in a 500-mL high-pressure stainless steel autoclave reactor (Baskerville, Manchester, U.K.). A volume of 350 mL of solvent was added to the reactor, followed by 2 g of 2-butyne-1,4-diol. The operating conditions of a reference reaction are displayed in Table 1. After filling, the reactor was closed, purged with nitrogen, and heated to the reaction temperature. The reactor

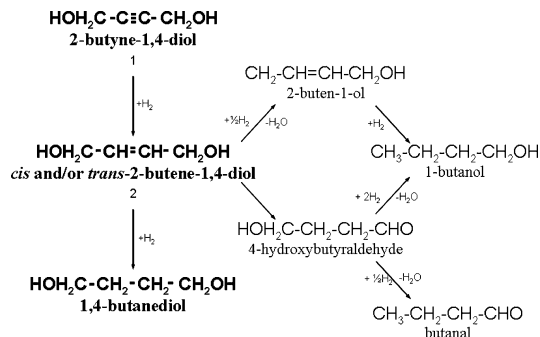


Figure 1. Reaction scheme for 2-butyne-1,4-diol hydrogenation. Boldface font indicates the preferred reaction pathway, with 2-butene-1,4-diol as the desired product.

then was opened, the catalyst was introduced, and the reaction started, by switching from a nitrogen gas flow to a hydrogen gas flow. The different parameters of the reaction were set on the control computer linked remotely to a hydrogen mass flow meter, pressure and temperature sensors, and reactor stirrer speed control. When the experiment started, the vessel was filled with hydrogen until the pressure inside it reached the set value. The reaction was run “dead-end” under pressure control, such that hydrogen consumed by the reaction was replenished by the controller to maintain the setpoint of the pressure. The sample pipe was purged with the reaction mixture before collecting any sample, to ensure that the liquid collected was representative of the mixture in the reactor and not a stagnant sample that had been left in the pipe.

Figure 1 displays the reaction network with the possible overhydrogenation and side products that may be formed under nonoptimal conditions. To compare the influence of different parameters on the speed and on the selectivity of the hydrogenation of 2-butyne-1,4-diol toward 2-butene-1,4-diol, the reactions were operated under different conditions. The effects of stirring speed (600–1400 rpm), and metal loading upon the catalyst support (5 and 25 wt %) were studied. When comparing different metal loadings upon the catalyst support, the same mass of metal was used in each case, and the mass of support therefore was reduced accordingly for the higher loaded catalyst. This method was considered to provide a rational basis for comparison of the two metal loadings. A comparison was also made between two different solvents, namely, pure 2-propanol and 5% 2-propanol in water. These two solvent compositions were chosen because it was previously demonstrated that 2-propanol exhibits maximum hydrogen solubility, while 5% 2-propanol in water displays the smallest hydrogen bubble size, leading to maximum interfacial surface area.²⁴

To further investigate the effects of gas–liquid and liquid–solid mass transfer in the reactor, selected reactions were performed with different catalyst loading in the reactor (0.05–0.4 g). For these reactions, a different strain of bacteria, *Rhodobacter capsulatus* (5 wt % Pd/R. *capsulatus*), was utilized, because this strain was available in more abundant supply than *A. oxidans* as a waste from another process and, thus, was able to supply the larger demand for catalyst required for the variable loading studies.

To check that the palladium metal had not leached from the bacterial biomass into solution, to act as a homogeneous catalyst, at the end of a selected reaction, the catalyst was separated from the reaction mixture using vacuum filtration, and the solvent from the first reaction was reused in a hydrogenation reaction, to which B3D was added without additional catalyst. The conditions used in this solvent recycling experiment were 2 g

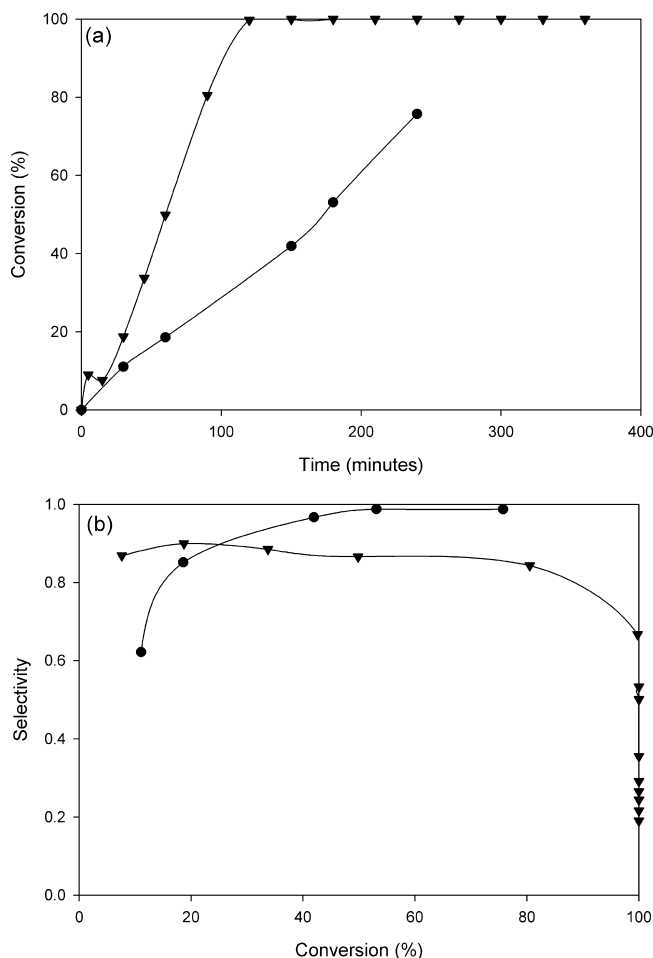


Figure 2. (a) Conversion of 2-butyne-1,4-diol versus time and (b) selectivity toward 2-butene-1,4-diol versus conversion of 2-butyne-1,4-diol in (▼) 100% 2-propanol and (●) 5% 2-propanol in water, using a 5 wt % Pd/A. *oxidans* catalyst. Unless otherwise stated, lines are shown to guide the eye.

of 2-butyne-1,4-diol, 285 mL of 2-propanol, and 15 mL of deionized water. The reactor was purged with nitrogen before heating the mixture to 40 °C with stirring (1000 rpm). Once at 40 °C, in the first run only, catalyst (0.100 g 5% Pd/R. *capsulatus*) was added; in both runs, the reactor was sealed and then pressurized with 2 bar of hydrogen.

Catalyst Characterization. CO chemisorption experiments were conducted on a Micromeritics Autochem II chemisorption analyzer with a thermal conductivity detector. The sample (0.5 g) was heated (10 °C/min) to 300 °C under H₂ (50 mL/min), then allowed to cool to 40 °C and stabilize before pulses of CO (loop volume = 0.5389 mL) were passed through the sample.

3. Results and Discussion

3.1. Effect of the Solvent. Initial studies were performed using Pd/A. *oxidans*. Figure 2a displays the conversion profiles of 2-butyne-1,4-diol (B3D), as a function of time in different solvents, whereas Figure 2b shows the selectivity behavior. It can be observed (Figure 2a) that the conversion rate in 100% 2-propanol was much faster than that for 5% v/v 2-propanol/water, with the conversion in the former case reaching 100% at a reaction time of 110 min, while the latter reached a conversion of 75% at 240 min, when the reaction stopped. The reason for the increased rate of reaction in 2-propanol is attributable to the higher solubility of hydrogen in the alcohol, compared with water.²⁴ Greater selectivity toward 2-butene-

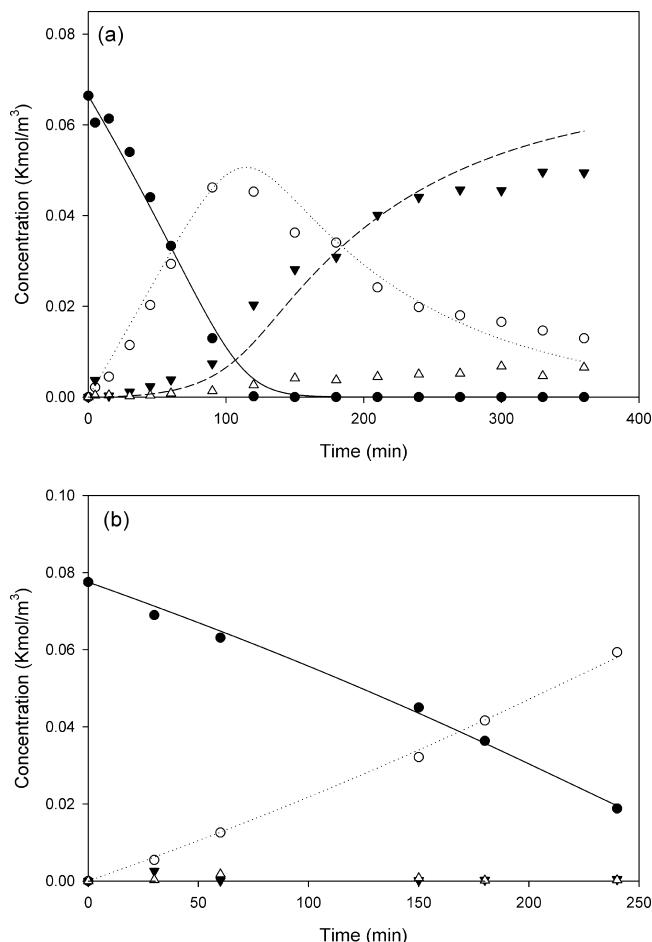


Figure 3. (a) Concentration profiles in 100% 2-propanol, (b) Concentration profiles in 5% 2-propanol in water using 5 wt % Pd/A. *oxidans* catalyst. Experimental data points: (●) B3D, (○) B2D, (▼) B1D, and (△) side products. Lines shown are the best fits of the model equations (eqs 1–3) to the experimental data points (—) B3D, (···) B2D, and (---) B1D.

1,4-diol (B2D) was obtained in the 2-propanol/water mixture (Figure 2b). As shown in Figure 1, several side products may form during the reaction; these are 2-buten-1-ol, 1-butanol, 4-hydroxybutyraldehyde, and butanal, and could also include 2-hydroxyhydrofuran and crotyl alcohol.^{19,28,29} Several side product peaks were detected during the reaction, including butanol, butyraldehyde, and crotyl alcohol; in Figure 3, these have been grouped as “side products”. A control reaction was performed over an *A. oxidans* catalyst support lacking Pd(0), which showed no conversion from the bacterial support without the presence of palladium nanoparticles, thus demonstrating the catalytic activity of the nanoparticles. Figure 3a displays the concentration profiles of the various components of the reaction, illustrating that, in the alcohol solvent, the concentration of 2-buten-1,4-diol (B2D) reaches a maximum at a reaction time of 100 min. By contrast, Figure 3b shows that the concentration of B2D increases monotonically without reaching a maximum at the time when the reaction was stopped. In a 2-propanol solvent (see Figure 3a), the amount of side products formed (i.e., those not accountable as B3D, B2D, or B1D) reached values up to 10.1% at a reaction time of 300 min. In contrast (Figure 3b), for 5% 2-propanol/water, the maximum concentration of side products was 2.6% at a reaction time of 60 min, and thereafter the amount of side products decreased. Therefore, it is concluded that side product formation occurred to a much greater extent in 2-propanol, compared to that in a mixed

solvent. Similar effects were previously observed by Fishwick et al.²¹ with a conventional Pd/Al₂O₃ catalyst for the same substrate and solvent system.

The performance of the BioPd catalysts under different conditions may be assessed in terms of reaction rate and selectivity toward B2D, which is the desirable product of the reaction. Selectivity toward B2D was calculated as the number of moles of 2-buten-1,4-diol divided by the total number of moles of all products detected, and hereafter references to selectivity relate to this value. Figure 2b illustrates the selectivity in the different solvents as a function of conversion, showing that selectivity in pure 2-propanol reached a maximum of ~0.9 at a conversion of ~19%, and selectivity and thereafter decreased to ~0.84 at ~80% conversion, before dropping rapidly at 100% conversion. By contrast, the selectivity for the mixed solvent increased to a maximum of 0.99 at ~75% conversion. In the pure 2-propanol, the rate of reaction is so fast that B3D is rapidly consumed, and the higher solubility of hydrogen also leads to overhydrogenation of B2D to produce 2-butane-1,4-diol (B1D). By contrast, in the mixed solvent, the hydrogenation is slower, and the lower hydrogen solubility means that hydrogen has a tendency to be used for the primary hydrogenation of B3D, rather than overhydrogenation of B2D. It was previously shown that BioPd catalysts can be recycled and reused,⁹ and, therefore, that palladium does not significantly leach from bacterial cells, and that the biomass are not destroyed by the solvent during the reaction. The absence of metal leaching was further checked by recycling the solvent from a reaction in a second run, to which fresh B3D but no additional supported catalyst was added. After 5 h of reaction time, no conversion of B3D was detected, thus demonstrating that the solvent did not contain homogeneous palladium, which had been leached from the catalyst during the previous reaction run.

Alkyne hydrogenation reactions typically follow Langmuir–Hinshelwood-type kinetic expressions of the type³⁰

$$R_1 = -\frac{dC_{B3D}}{dt} = \frac{mk_1C_{H_2}C_{B3D}}{(1 + K_{B3D}C_{B3D} + K_{B2D}C_{B2D})^2} \quad (1)$$

For the alkene hydrogenation, the rate is given by

$$R_2 = \frac{mk_2C_{H_2}C_{B2D}}{(1 + K_{B3D}C_{B3D} + K_{B2D}C_{B2D})^2} \quad (2)$$

Thus, the rate of consumption of alkene is determined by the difference of the aforementioned rates:

$$\frac{dC_{B2D}}{dt} = R_1 - R_2 \quad (3)$$

The rate of production of alkane is found from the rate of consumption of alkene:

$$\frac{dC_{B1D}}{dt} = R_2 \quad (4)$$

For the reactions in each solvent, eqs 1–3 were fitted to the experimental data points, to minimize the sum of the squares of the difference between experimental and calculated points for B3D and B2D simultaneously, using a solver function of MS Excel software. A constraint was imposed that the coefficients must be greater than or equal to zero. The concentration of hydrogen in 5% 2-propanol/water was assumed to be approximately equal to the value predicted by Henry’s law in water (0.0014 kmol/m³),³¹ while the dissolved concentration of

Table 2. Values of Rate and Adsorption Constants (eqs 1 and 2), Determined by Fitting eqs 1–3 to the Experimental Data Shown in Figure 3

	k_1 ((m ³) ² /kmol kg s)	K_{B3D} (m ³ /kmol)	k_2 ((m ³) ² /kmol kg s)	K_{B2D} (m ³ /kmol)
100% 2-propanol	0.51	31.28	3.41	0.00
5% 2-propanol in water	2.16	51.40	0.00	3.02

hydrogen in 2-propanol was determined by Hu et al.²⁴ to be ~ 6 times higher than the dissolved concentration in water and, thus, was used to estimate the concentration of hydrogen in 2-propanol (0.0084 kmol/m³). The catalyst loading used was 0.29 kg/m³, while the initial concentration of B3D ($C_{B3D}(t=0)$) was equal to 0.0664 kmol/m³. The fitted values of the kinetic and adsorption parameters are shown in Table 2, and the lines shown in Figures 3a and 3b display the calculated concentration profiles for the same fitted constants. The initial rate of reaction calculated for the first 60 min of reaction time was 8.33×10^{-6} Kmol/(mm³ s) for 2-propanol, whereas for the mixed solvent, the initial rate was 3.33×10^{-6} Kmol/(mm³ s), approximately 2.5 times slower than for the pure alcohol. Approximate calculation of the diffusion coefficient of hydrogen in 2-propanol from the Wilke Chang equation³² at the reaction temperature gave a value of 2.86×10^{-9} m²/s, while in water, the value was very similar (2.89×10^{-9} m²/s). Therefore, the solubility of hydrogen has more influence on the reaction rate than the diffusivity.

As shown in Figure 3a, the calculated concentration profiles follow the trends in experimental values quite closely, up to ~ 200 min of the experiment for the 100% 2-propanol solvent. The calculated values of B3D concentration show a good agreement at all times, and for B2D, the calculated values are slightly higher than the experimental values at ~ 100 –150 min and are slightly lower at times greater than 300 min. For B1D, the calculated values are slightly lower than the experimental values at 100–150 min and slightly higher at greater than 300 min. In Figure 3b, the calculated and experimental values for B3D and B2D display good agreement at all times; however, because of the slow rate of reaction, the maximum B2D concentration is not attained, and negligible amounts of B1D are formed. Because little hydrogenation of B2D occurs in 5% 2-propanol in water, the value of k_2 is predicted to be zero in Table 2. The predicted adsorption coefficient K_{B3D} (see Table 2) is higher for the mixed solvent than for 100% 2-propanol. Similarly, K_{B2D} is predicted to be higher in the mixed solvent and zero in pure 2-propanol. Although one must be cautious of overinterpreting a mathematically fitted value, the predicted K_{B2D} value in pure 2-propanol suggests that adsorption of the alkene does not occur in the pure alcohol. These calculated adsorption coefficients are consistent with experimental studies of the adsorption coefficient that have been performed for the pentyne/pentene system over a Pd/Al₂O₃ catalyst by Bennett et al.³³ In their work, adsorption experiments were conducted to determine the change in concentration of a 2-pentyne or 2-pentene solution after being allowed to equilibrate with a high loading of Pd/Al₂O₃ catalyst for 1 h at 40 °C. The concentration of alkyne in 2-propanol fell by $\sim 11\%$, whereas the amount of 2-pentene in 2-propanol showed only a small decrease in concentration (~ 5 times less than that observed with the alkyne). Taken together, the calculated adsorption coefficient for B2D and the previously measured coefficient for 2-pentene confirm that alkene adsorption upon palladium is much lower than alkyne adsorption, and this can help to explain why alkane production only starts to occur significantly once all of the alkyne has been consumed from the solution. In the present study, the mathematical form of the rate equation described in eq 1 suggests that, in the limiting cases, at low concentrations of B3D, first-order behavior would occur. At high B3D concentrations, a negative reaction

order in B3D may result, as reported by Moulijn et al.,³⁴ which is attributable to the adsorption of B3D on the catalyst, thus preventing the adsorption of hydrogen and slowing the reaction.

3.2. Effect of Stirring Speed. Figures 4a and 4b respectively display the conversion and selectivity profiles for three different stirring speeds: 600, 1000, and 1400 rpm. It can be observed that the rate of conversion at 600 rpm is significantly slower than the rates at 1000 and 1400 rpm, which are almost the same. Therefore, it can be deduced that, at the lower stirring speed, the reaction is mass-transfer-limited. As demonstrated in Figure 4a, the reaction rate is not significantly influenced by stirring speed at values above 1000 rpm. Because of the very small bacterial particle size (~ 4 μ m), it is unlikely that internal or external resistances to mass transfer at the catalyst particle would play a significant role in limiting the reaction rate; thus, at lower stirring speeds, gas–liquid mass-transfer resistance is thought to be significant.

Interestingly, Figure 4b shows that the selectivity decreases with stirring speed. Since less hydrogen is transported to the catalyst surface at lower stirring speed, because of the lower mass-transfer rate, less overhydrogenation of B2D to B1D occurs. Consequently, selection of the stirring speed for the

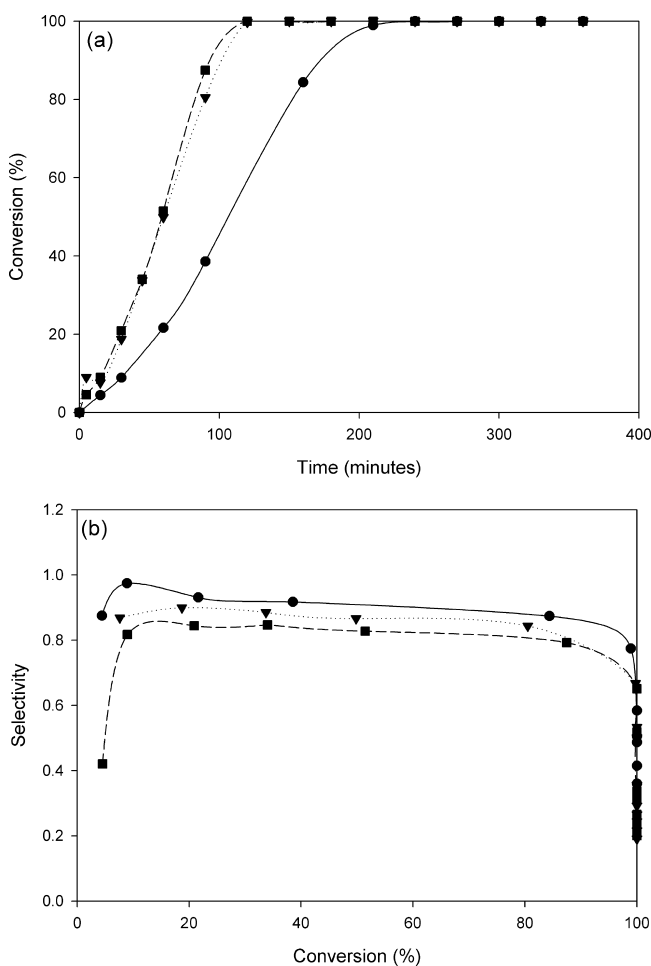


Figure 4. Plots of (a) conversion versus time and (b) selectivity versus conversion of B3D and selectivity toward B2D profiles for stirring speeds of 600, 1000, and 1400 rpm, using 5 wt % Pd/A. *oxidans* catalyst. (Legend: (●) 600 rpm, (▼) 1000 rpm, and (■) 1400 rpm.)

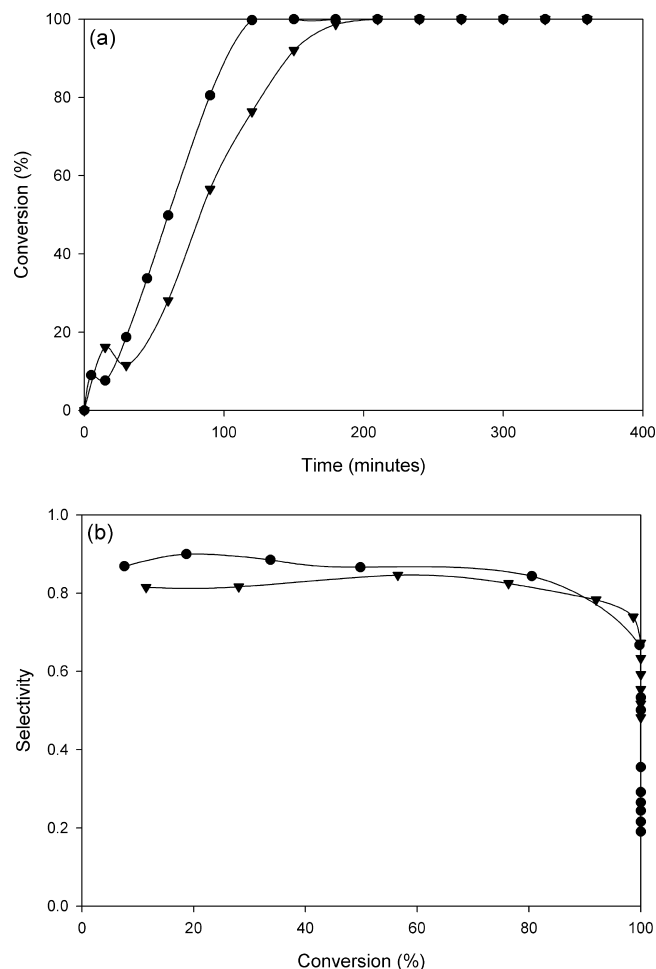


Figure 5. Plots of (a) conversion versus time and (b) selectivity versus conversion profiles for different catalyst loadings. (Legend: (●) 5 wt % Pd/A. *oxidans* and (▼) 25 wt % Pd/A. *oxidans*.)

reaction permits a tradeoff between high selectivity and high reaction rate.

3.3. Effect of Metal Loading on the Catalyst. Similar to conventionally supported catalysts, it is possible to prepare the BioPd with different metal loadings. To study the effect of metal loading, two different catalyst samples were prepared, with palladium loadings of 5 and 25 wt %. To compare the reactions with the two catalysts, the same molar ratio of Pd/substrate (0.205 mol %) Pd was maintained in both reactions, by reducing the amount of the catalyst with higher palladium loading in the reaction.

Figure 5a shows that the rate of reaction is slower for the catalyst with higher metal loading. As shown in Figure 5b, the selectivity is slightly higher for the 5% Pd catalyst at conversions in the range of ~15%–85%, although the selectivity decays below that of the 25% Pd catalyst at 100% conversion, because overhydrogenation to B1D occurs. The results of CO pulse chemisorption showed that the metal particle size of the 5 wt % BioPd was 2 nm, whereas the 25 wt % BioPd had a metal particle size of 30 nm. Consequently, the 5 wt % material had a higher dispersion of metal, which has a tendency to lead to a higher rate of reaction, which is attributable to the accessibility of reactants to active metal centers. However, the higher selectivity for the 25 wt % catalyst is due to two possible factors. First, the lower accessible surface and, therefore, slower rate of hydrogenation has a tendency to limit the extent of overhydrogenation of B2D to B1D, compared to the lower-loaded catalyst. Second, the relatively large metal clusters on the

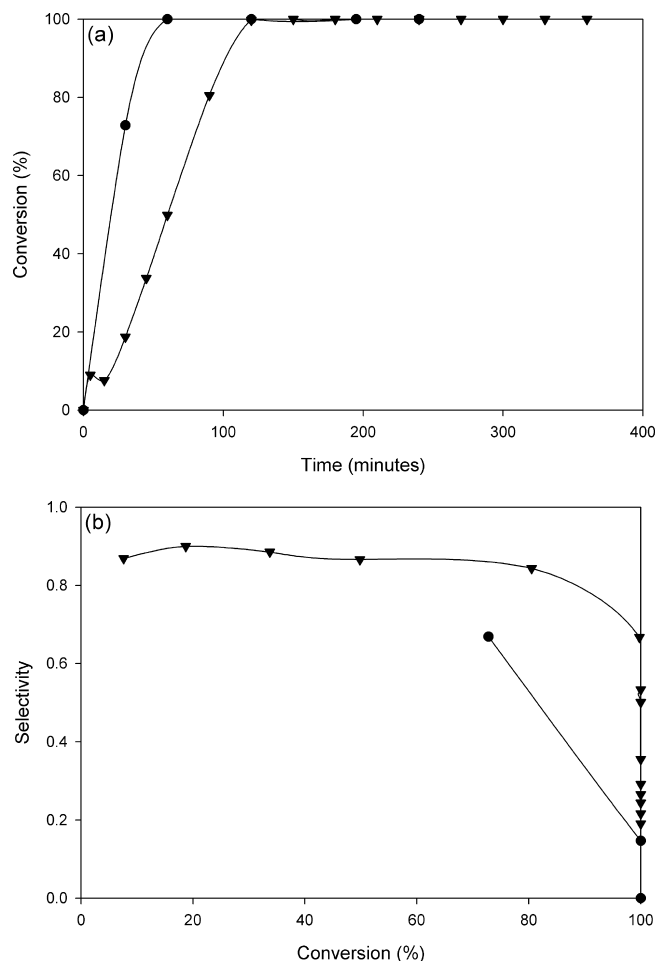


Figure 6. Plots of (a) conversion versus time and (b) selectivity versus conversion for (▼) 5 wt % Pd/A. *oxidans* and (●) 5 wt % Pd/Al₂O₃.

catalyst have a higher ratio of plane surfaces to terraces and edges, which has a tendency to favor adsorption modes that lead to less formation of side products.^{35,36} These results are supported by the findings of Doyle et al.,^{37,38} which indicate that alkene hydrogenation is faster on larger particles. This would suggest that the 25% Pd catalyst with larger particle size would lead to a higher rate of hydrogenation of B2D to B1D and, thus, lower selectivity to B2D, compared to smaller particles, as observed at conversions of <85%. To selectively hydrogenate B3D to B2D, it is important to suppress highly active subsurface hydrogen, to prevent excessive alkane formation. A further study³⁹ found that smaller particles are likely to be unselective in alkyne hydrogenation, resulting in alkane production. In the present work, this effect is not observed at low conversions of B3D; however, at higher conversions (>85%), significant B1D production does occur.

3.4. Comparison of BioPd with Commercial Catalyst. To assess whether the BioPd catalyst could be used in place of existing catalysts, comparison was made with a typical industrial catalyst, consisting of 5 wt % Pd/Al₂O₃. The conversion selectivity profiles for 5 wt % Pd/A. *oxidans* and the conventional catalyst are shown in Figures 6a and 6b. It is observed that the rate is slower for the BioPd, but the selectivity is considerably better than that for the conventional catalyst. Making a comparison at the same conversion of 73%, the selectivity for Pd/Al₂O₃ is ~0.67, whereas, from the best-fit trendline interpolating between the data points, for Pd/A. *oxidans*, the selectivity is ~0.85. The palladium particle diameter, as determined by CO pulse chemisorption, is 1.8 nm

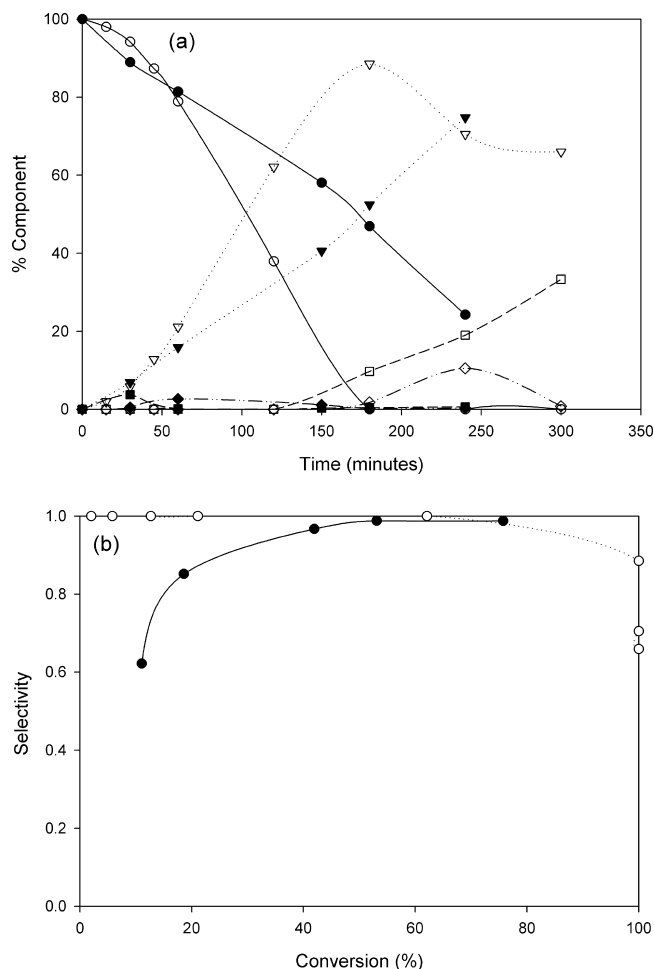


Figure 7. (a) Plot of conversion versus time; open symbols represent data for 5 wt % Pd/*R. capsulatus*, and filled symbols represent data for 5 wt % Pd/*A. oxidans* ((circles) B3D, (inverted triangles) B2D, (squares) B1D, and (diamonds) side products). (b) Plot of selectivity versus conversion for 5 wt % Pd/*R. capsulatus* and 5 wt % Pd/*A. oxidans*; open symbols represent data for *R. capsulatus*, and filled symbols represent data for *A. oxidans*.

for 5 wt % Pd/Al₂O₃, which is quite similar to the result of 2 nm for 5 wt % Pd/*A. oxidans*. Therefore, metal particle size effects do not seem to be the controlling factor in explaining the selectivity differences that are observed. A significant difference between BioPd and conventionally supported catalysts are that, in BioPd, the palladium particles are dispersed and stabilized throughout the outer layers of the cell, as described by Creamer.⁸ It is suggested that a diffusion of reactants into this layer must occur for adsorption to palladium and, thus, catalytic reactions to happen. This process may help to control the rate of hydrogenation and therefore limit the amount of overhydrogenation of B2D that occurs, as well as reduce the formation of side products. Thus, in addition to supporting and stabilizing the nanoparticles, the surface layers of the dried bacterial cells persist to assist in catalytic selectivity to a greater extent than would normally occur in classical manufacturing of chemical catalysts.

3.5. Effect of Bacterial Strain and Analysis of Mass-Transfer Effects. A comparison was made between the catalytic activity and selectivity for the two different strains of bacteria used in the experiments, comparably loaded with palladium at 5 wt % of the bacterial dry weight (*A. oxidans* and *R. capsulatus*). Component reaction profiles for these two catalysts are displayed in Figure 7a. It was observed that the rate of decay of B3D concentration for *R. capsulatus* was

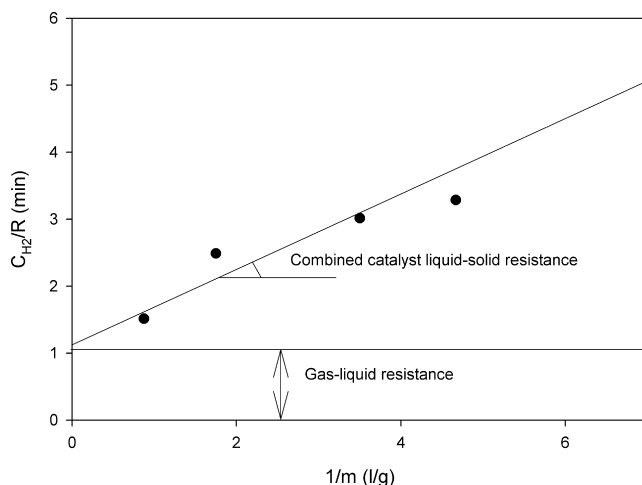


Figure 8. Plot of C_{H_2}/R_{H_2} versus $1/m$ for 5 wt % Pd/*R. capsulatus* catalyst, used to facilitate determination of gas-liquid and liquid-solid mass-transfer resistances in the reactor. Symbols denote experimental data, and the line shown represents a linear regression to the data.

initially slower than that of *A. oxidans*; however, after 60 min, it accelerated such that the trend was reversed. The peak concentration of B2D (88.5%) occurred at 180 min for *R. capsulatus*; however, after 240 min, a peak concentration for B2D with Pd/*A. oxidans* catalyst had not yet been reached. Toward the end of the reaction, the amount of alkane produced was higher for the Pd/*R. capsulatus*. Figure 7b displays the selectivity observed at different conversions, and it shows that, for Pd/*R. capsulatus*, 100% selectivity was maintained up to at least 62% conversion, and only decreased at 100% conversion, whereas for Pd/*A. oxidans*, the selectivity showed an increase with conversion up to ~0.99 at 75.7% conversion. Hence, this study suggests that Pd(0) held on the more-complex Gram-negative cell wall may be superior, in terms of reaction rate and selectivity, than that supported on Gram-positive bacteria. A previous study (by Creamer et al.⁸) suggested that, in the hydrogenation of itaconic acid, both cell types performed comparably but at slightly different optimal palladium loadings in each case. Further studies comparing different Gram-positive and Gram-negative bacteria will be performed and published in the future.

In slurry reactors, the various resistances to mass transfer at the gas/liquid and liquid/solid interfaces, and internal resistance within the catalyst particle, may be expressed according to the equation^{40,41}

$$\frac{C_{A_i}}{R_A} = \frac{1}{k_b a_b} + \frac{1}{m} \left(\frac{1}{k_l a_l} + \frac{1}{\eta k} \right) \quad (5)$$

Thus, by regressing eq 5 to experimental data (Figure 8) for C_A/R_A versus $1/m$, the various mass-transfer resistances may be estimated from the slope and intercept of the plot. To construct such a plot for the hydrogenation reaction over the Pd/*R. capsulatus* catalyst in 5% 2-propanol/water, the concentration of hydrogen at the interface (C_{A_i}) was approximated as being equal to the saturation value in water at the same temperature and pressure. The saturated hydrogen concentration was calculated from Henry's law³¹ as 0.0014 kmol/m³. Reaction rates were calculated by regression of the line of best fit to the concentration-time data, up to the first 20 min of reaction time, assuming that, for the initial data, one mole of hydrogen reacts with one mole of B3D. The resulting plot of C_{A_i}/R_A is shown in Figure 8, from which the intercept ($1/k_b a_b$) is 1.12 min, the

slope ($1/k_1a_l + 1/\eta k$) is 0.56 min g/L, and $R^2 = 0.94$ for the fit. The gas–liquid resistance may be estimated from the value of the intercept and the combined resistance at the catalyst particle from the slope of the regression line. The percentage contributions of the gas–liquid (G-L) and liquid–solid (L-S) resistances to the value of C_A/R_A change with catalyst loading. At a particular catalyst loading, the contribution from the liquid–solid resistance may be calculated as the difference between the value of C_A/R_A at that loading minus the value of the intercept, and, thus, the percentage contribution of each resistance calculated. For example, at the highest catalyst loading ($1/m = 0.875$), 25.8% of the resistance is due to the L-S mass-transfer step and 74.2% is due to the G-L mass-transfer step; at the lowest loading ($1/m = 7.0$), the resistances are 78.9% (L-S) and 21.1% (G-L); and, at a typical intermediate loading ($1/m = 3.5$), the resistances are 62.8% (L-S) and 37.2% (G-L).

4. Conclusions

To evaluate a new class of palladium catalysts made via the reduction of Pd(II) onto bacterial cell surfaces, in comparison to chemically manufactured counterparts, the selective hydrogenation of 2-butyne-1,4-diol to 2-butene-1,4-diol was studied. The reaction was performed in a 500-mL stirred tank reactor, and the reaction conditions were varied to study the selectivity toward 2-butene-1,4-diol and determine the optimal conditions for the production of this component.

The optimization results showed that, under some conditions, there was a tradeoff between obtaining a fast reaction rate and a high selectivity. Solvent selection influences the reaction rate, and it was determined that a mixture of 5% 2-propanol in water led to higher selectivity than 100% 2-propanol, although the rate was faster in pure 2-propanol. The concentration profiles of reactants and products, as a function of time, were fitted satisfactorily using a Langmuir–Hinshelwood expression. Adjustment of the stirring speed also affected the rate and selectivity, such that the rate increased at a critical value of ~1000 rpm, because of the elimination of gas–liquid mass-transfer limitation. Further analysis of gas–liquid and liquid–solid mass-transfer resistances was performed for different catalyst loadings. This is the first time such an analysis has been conducted in a hybrid biochemical system, although such studies are commonplace in “traditional” reaction engineering. Selection of a suitable gas sparger and careful agitator design in the reactor can be used to reduce the resistances to mass transfer and thus optimize the reactor behavior.

BioPd was compared with a conventionally supported catalyst (5 wt % Pd/Al₂O₃) and gave a higher selectivity in the reaction, despite a slightly lower reaction rate for the same operating conditions. Therefore, BioPd seems to be a promising catalyst/support system for conducting selective hydrogenation reactions. Comparison of two different bacterial strains (*A. oxidans* and *R. capsulatus*) showed relatively small differences in rate and both demonstrated good (~0.99–1) maximum selectivity toward B2D. Because the use of bacteria facilitates the inexpensive manufacture of catalysts from metal-waste-bearing solutions (for example, from the electronics and automotive industries), this new approach could offer a cost-effective solution to the problem of providing selective supported catalysts.

Nomenclature

Variables

a = interfacial area

C = concentration of component

k = reaction rate constant

k_b = gas–liquid mass-transfer coefficient at gas bubble boundary

k_l = liquid–solid mass-transfer coefficient

K = adsorption coefficient

m = catalyst loading

R = rate of reaction

Abbreviations

B1D = 2-butane-1,4-diol

B2D = 2-butene-1,4-diol

B3D = 2-butyne-1,4-diol

Pd/*A. oxidans* = Pd(0) made on the surface of *A. oxidans* cells and dried

Pd/*R. capsulatus* = Pd(0) made on the surface of *R. capsulatus* cells and dried

Greek Letters

η = catalyst effectiveness factor

Subscripts

A = component A

b = gas–liquid, or gas bubble

H₂ = hydrogen

i = interface

l = liquid–solid

1 = eq 1

2 = eq 2

Acknowledgment

The authors acknowledge funding of the project from the Biotechnology and Biological Sciences Research Council (BB-SRC BB/E003788/1) and the Engineering and Physical Sciences Research Council (EPSRC EP/D05768X/1), UK. We thank Dr. Zhihua Zhou (Laboratory of Molecular Microbiology, Institute of Plant Physiology and Ecology, Shanghai Institutes for Biological Sciences, Chinese Academy of Sciences, Shanghai, PRC) for the donation of the bacterial strain *R. capsulatus* (ZX-5). We also thank Dr. M. D. Redwood and Mr. R. Orozco (University of Birmingham) for growing and supplying the *R. capsulatus* biomass that was used in this study.

Literature Cited

- (1) Eberhardt, W. Clusters as new materials. *Surf. Sci.* **2000**, *500*, 242.
- (2) Hori, H.; Teranishi, T.; Nakae, Y.; Seino, Y.; Miyake, M.; Yamada, S. Anomalous Magnetic Polarization Effect of Pd and Au Nano-Particles. *Phys. Lett. A* **1999**, *263*, 405.
- (3) Lloyd, J. R.; Yong, P.; Macaskie, L.E. Enzymatic Recovery of Elemental Palladium by Using Sulfate-Reducing Bacteria. *Appl. Environ. Microb.* **1998**, *64*, 4608.
- (4) Macaskie, L. E.; Yong, P.; Paterson-Beedle, M.; Thrackray, A. C.; Marquis, P. M.; Sammons, R. L.; Nott, K. P.; Hall, L.D. A Novel Non Line-Of-Sight Method For Coating Hydroxyapatite onto the Surfaces of Support Materials by Biomineralization. *J. Biotechnol.* **2005**, *118*, 187.
- (5) Creamer, N. J.; Baxter-Plant, V. S.; Henderson, J.; Potter, M.; Macaskie, L. E. Palladium and Gold Removal and Recovery from Precious Metal Solutions and Electronic Scrap Leachates by *Desulfovibrio desulfuricans*. *Biotechnol. Lett.* **2006**, *28*, 1475.
- (6) Mabbett, A. N.; Sanyahumbi, D.; Yong, P.; Macaskie, L. E. Biorecovered Precious Metals from Industrial Wastes: Single-Step Conversion of a Mixed Metal Liquid Waste to a Bioinorganic Catalyst with Environmental Application. *Environ. Sci. Technol.* **2006**, *40*, 1015.
- (7) Mikheenko, I. P. Nanoscale Palladium Recovery, Ph.D. Thesis, The University of Birmingham, Birmingham, U.K., 2004.
- (8) Creamer, N. J.; Mikheenko, I. P.; Yong, P.; Deplanche, K.; Sanyahumbi, D.; Wood, J.; Pollmann, K.; Merroun, M.; Selenska-Pobell, S.; Macaskie, L. E. Novel Supported Pd Hydrogenation Bionanocatalyst for Hybrid Homogeneous/Heterogeneous Catalysis. *Catal. Today* **2007**, *128*, 80.

- (9) Bennett, J. A.; Creamer, N. J.; Deplanche, K.; Macaskie, L. E.; Shannon, I.; Wood, J. Palladium Supported on Bacterial Biomass as a Novel Heterogeneous Catalyst: A Comparison of Pd/Al₂O₃ and Bio-Pd in the Hydrogenation of 2-Pentyne. *Chem. Eng. Sci.* In press, **2009**, DOI: 10.1016/j.ces.2009.06.069.
- (10) Baxter-Plant, V. S.; Mikheenko, I. P.; Macaskie, L. E. Sulphate-Reducing Bacteria, Palladium and the Reductive Dehalogenation of Chlorinated Aromatic Compounds. *Biodegradation* **2003**, *14*, 83.
- (11) De Windt, W.; Aelterman, P.; Verstraete, W. Bioreductive Desorption of Palladium(0) Nanoparticles on *Schewanella Oneidensis* with Catalytic Activity Towards Reductive Dechlorination of Polychlorinated Biphenyls. *Environ. Microbiol.* **2005**, *7*, 314.
- (12) Mertens, B.; Blothe, C.; Windey, K.; De Windt, W.; Verstraete, W. Biocatalytic Dechlorination of Lindane by Nano-scale Particles of Pd(0) Deposited on *Schewanella Oneidensis*. *Chemosphere* **2007**, *66*, 99.
- (13) Harrad, S.; Robson, M.; Hazrati, S.; Baxter-Plant, V. S.; Deplanche, K.; Redwood, M. D.; Macaskie, L. E. Dehalogenation of Polychlorinated Biphenyls and Polybrominated Diphenyl Ethers Using a Hybrid Bioinorganic Catalyst. *J. Environ. Monitor.* **2007**, *9*, 314.
- (14) Deplanche, K.; Snape, T. J.; Hazrati, S.; Harrad, S.; Macaskie, L. E. Versatility of a New Bioinorganic Catalyst: Palladized Cells of *Desulfovibrio desulfuricans* and Application to Dehalogenation of Flame Retardant Materials. *Environ. Technol.* **2009**, *30* (7), 681.
- (15) Mabbett, A. N.; Yong, P.; Farr, J. P. G.; Macaskie, L. E. Reduction of Cr(VI) by "Palladized"-Biomass of *Desulfovibrio desulfuricans*. *Bio-technol. Bioeng.* **2004**, *90*, 589.
- (16) Natividad, R.; Cruz-Olivares, J.; Fishwick, R. P.; Wood, J.; Winterbottom, J. M. Scaling Out Selective Hydrogenation Reactions: From Single Capillary to Monolith. *Fuel* **2007**, *86*, 1304.
- (17) Chaudhari, R. V.; Parande, M. G.; Ramachandran, P. A.; Brahme, P. H.; Vadgaonkar, H. G.; Jaganathan, R. Hydrogenation of Butynediol to Cis-Butenediol Catalyzed by Pd-Zn-CaCO₃: Reaction Kinetics and Modeling of a Batch Slurry Reactor. *AIChE J.* **1985**, *31*, 1891.
- (18) Telkar, M. M.; Rode, C. V.; Rane, V. H.; Jaganathan, R.; Chaudhari, R. V. Selective Hydrogenation of 2-butyne-1,4-diol to 2-butene-1,4-diol: roles of ammonia, catalyst pretreatment and kinetic studies. *Appl. Catal., A* **2001**, *216*, 13.
- (19) Turek, F.; Winter, H. Effectiveness Factor in a Three-Phase Spinning Basket Reactor: Hydrogenation of Butynediol. *Ind. Eng. Chem. Res.* **1990**, *29*, 1546.
- (20) Marwan, H.; Winterbottom, J. M. The Selective Hydrogenation of Butyne-1,4-diol by Supported Palladiums: A Comparative Study on Slurry, Fixed Bed and Monolith Downflow Bubble Column Reactors. *Catal. Today* **2004**, *97*, 325–330.
- (21) Fishwick, R. P.; Natividad, R.; Kulkarni, R.; McGuire, P. A.; Wood, J.; Winterbottom, J. M.; Stitt, E. H. A Comparative Study of Monolith CDC, Stirred Tank and Trickle Bed Reactors. *Catal. Today* **2007**, *128*, 108.
- (22) Joannet, E.; Horny, C.; Kiwi-Minsker, L.; Renken, A. Palladium Supported on Filamentous Active Carbon as Effective Catalyst for Liquid-Phase Hydrogenation of 2-Butyne-1,4-diol to 2-butene-1,4-diol. *Chem. Eng. Sci.* **2002**, *57*, 3453.
- (23) Kiwi-Minsker, L.; Joannet, E.; Renken, A. Solvent-Free Selective Hydrogenation of 2-Butyne-1,4-diol over Structured Palladium Catalyst. *Ind. Eng. Chem. Res.* **2005**, *44*, 6148.
- (24) Hu, B.; Fishwick, R. P.; Pacey, A. W.; Winterbottom, J. M.; Wood, J.; Stitt, E. H.; Nienow, A. W. Simultaneous Measurement of *In-Situ* Bubble Size and Reaction Rates with a Heterogeneous Catalytic Hydrogenation Reaction. *Chem. Eng. Sci.* **2007**, *62*, 5392.
- (25) Khalfaoui, B.; Meniai, A. H.; Borja, R. Thermodynamic Properties of Water + Normal Alcohols and Vapor-Liquid Equilibria for Binary Systems of Methanol or 2-propanol with Water. *Fluid Phase Equilib.* **1997**, *127*, 181.
- (26) Sato, T.; Buchner, R. The Cooperative Dynamics of the H-bond System in 2-Propanol/Water Mixtures: Steric Hindrance Effects of Nonpolar Head Group. *J. Chem. Phys.* **2003**, *119*, 10789.
- (27) Dougan, L.; Bates, S. P.; Hargreaves, R.; Fox, J. P.; Crain, J.; Finney, J. L. Methanol–Water Solutions: A Bi-percolating Liquid Mixture. *J. Chem. Phys.* **2004**, *121*, 6456.
- (28) Musolino, M. G.; Cutrupi, C. M. S.; Donato, A.; Pietropaolo, D.; Pietropaolo, R. Liquid Phase Hydrogenation of 2-butyne-1,4-diol and 2-butene-1,4-diol Isomers over Pd Catalysts: Roles of Solvent, Support and Proton on Activity and Products Distribution. *J. Mol. Catal. A—Chem.* **2003**, *195*, 147.
- (29) Winterbottom, J. M.; Marwan, H.; Viladevall, J.; Sharma, S.; Raymahasay, S. Selective Catalytic Hydrogenation of 2-butene-1,4-diol to cis-2-butene-1,4-diol in Mass Transfer Efficient Slurry Reactors. *Stud. Surf. Sci. Catal.* **1997**, *108*, 59.
- (30) Rode, C. V.; Tayade, P. R.; Nadgeri, J. M.; Jaganathan, R.; Chaudhari, R. V. Continuous Hydrogenation of 2-Butyne-1,4-Diol to 2-Butene- and Butane-1,4-Diols. *Org. Process Res. Dev.* **2006**, *10*, 278.
- (31) Sander, R. Compilation of Henry's Law Constants for Inorganic and Organic Species of Potential Importance in Environmental Chemistry (Version 3), 1999. Available via the Internet at <http://www.henrys-law.org>.
- (32) Reid, R. C.; Prausnitz, J. M.; Poling, B. E. *The Properties of Gases and Liquids*, 4th Edition; McGraw–Hill: New York, 1987.
- (33) Bennett, J. A.; Fishwick, R. P.; Spence, R.; Wood, J.; Winterbottom, J. M.; Jackson, S. D.; Stitt, E. H. Hydrogenation of 2-pentyne over Pd/Al₂O₃ catalysts: Effect of operating variables and solvent selection. *Appl. Catal., A* **2009**, *364*, 57.
- (34) Moulijn, J. A.; Kapteijn, F.; van Santen, R. A.; Wever, R. Chemical Kinetics of Catalysed Reactions. In *Catalysis: An Integrated Approach*; van Santen, R. A., van Leeuwen, M. N., Moulijn, J. A., Averill, B. A., Eds.; Elsevier: Amsterdam, 1999; pp 81–106.
- (35) Freund, H. J.; Libuda, J.; Baumer, M.; Risse, T.; Carlsson, A. Clusters, Facets and Edges: Site-Dependent Selective Chemistry on Model Catalysts. *Chem. Rec.* **2003**, *3*, 181.
- (36) Jackson, S. D.; Doyle, A. M.; Shikhutdinov, S. K. Hydrogenation on Metal Surfaces: Why are Nanoparticles More Active than Single Crystals. *Angew. Chem., Int. Ed.* **2003**, *42*, 5240.
- (37) Doyle, A. M.; Shikhutdinov, S. K.; Freund, H.-J. Alkene chemistry on the palladium surface: nanoparticles vs single crystals. *J. Catal.* **2004**, *223*, 444.
- (38) Doyle, A.; Shikhutdinov, S. K.; Freund, H.-J. Surface-Bonded Precursor Determines Particle Size Effects for Alkene Hydrogenation on Palladium. *Angew. Chem., Int. Ed.* **2005**, *44*, 629.
- (39) Teschner, D.; Vass, E.; Hävecker, M.; Zafeirotas, S.; Schnörch, P.; Sauer, H.; Knop-Gericke, A.; Schlögl, R.; Chamam, M.; Wootsch, A.; Canning, A. S.; Gamman, J. J.; Jackson, S. D.; McGregor, J.; Gladden, L. F. Alkyne hydrogenation over Pd catalysts: A new paradigm. *J. Catal.* **242**, 26–37.
- (40) Winterbottom, J. M., King, M. B., Eds. *Reactor Design for Chemical Engineers*; Stanley Thorne: Cheltenham, U.K., 1999.
- (41) Fogler, H. S. *Elements of Chemical Reaction Engineering*, 4th Edition; Prentice Hall PTR: Upper Saddle River, NJ, 2006.

Received for review April 25, 2009

Revised manuscript received September 26, 2009

Accepted September 29, 2009

IE900663K